J. Am. Chem. Soc. **1993,** *115,* 6391–6397 6391

Photosubstitution of Iron Carbonyl Phosphine Complexes: Quantum Yield, Kinetic, and Thermochemical Studies

Suresh K. Nayak and Theodore J. Burkey*

Contribution from the Department of Chemistry, Memphis State University, Memphis, Tennessee 38152-0001

Received November 30, 1992

Abstract: The quantum yields and thermochemistry of photosubstitution of $Fe(CO)_4PR_3$ and $Fe(CO)_3(PR_3)_2$ (R = alkyl) in cyclohexane at 337 nm have been determined for the first time. In addition, time-resolved experiments provided the kinetics of the second step of the substitution, phosphine reaction with the intermediate formed upon CO dissociation. Several interesting results, with implications for understanding the interaction of probe molecules with potentially reactive metals centers, were noted. First, the quantum yields of photosubstitution of $Fe(CO)_4PR_3$ (R = Me, Et, and *n*-Bu, **1a–c**, respectively) with PR_3 are 0.56, 0.54, and 0.62 (R is the same for coordinated and dispersed ligand). Second, analysis of the products after photolysis of **1** with dispersed $(CH_3)_3CNC$ or CO indicates that coordinated CO substitutes but not PR_3. Third, the photolysis of $Fe(CO)_3(PMe_3)_2$ (**2**) with PMe_3 results in the substitution of CO ($\Phi = 0.50$), while photolysis with CO results in the substitution of PMe_3 ($\Phi = 0.03$). On the other hand, the photolysis of $Fe(CO)_3(dmpe)$ (**3**, dmpe = 1,2-bis(dimethylphosphino)ethane) with PMe_3 results in the substitution of only CO ($\Phi = 0.47$). Fourth, the enthalpies of CO dissociation in cyclohexane (ΔH_1) for **1a**, **1b**, **2**, and **3** were 40, 39, 30, and 36 kcal/mol, respectively, clearly indicating the change of the M–CO interaction caused by the phosphine ligand. Likewise, enthalpies of PR_3 addition (structure of attacking PR_3 is the same as the coordinated PR_3) to the intermediate formed after CO dissociation (ΔH_2) were 41, 46, 20, and 33 kcal/mol, respectively. These results lead to the conclusion that the $Fe(CO)_3(PR_3)$–L bond is about the same strength for L = CO and PR_3, while the $Fe(CO)_2(PR_3)_2$–L bond is weaker for L = PR_3 than for CO. The latter finding is counter to simple electronic arguments based on relative π-acidity of ligands. The thermochemical and kinetic trends point out the importance of steric effects in modulating ligand dissociation and addition at a metal center.

Introduction

Understanding the thermodynamics and kinetics of probe molecule (*e.g.* H_2, RH, CO, and PR_3) reactions with transition-metal centers is crucial to the rational design of improved catalysts.[1] The C–H activation of alkanes by a transition-metal catalyst is a reaction of great potential use; thus, we became interested in the thermochemistry of iron phosphine compounds when $Fe(dmpe)_2(H)(n\text{-}C_5H_{11})$ was reported to form upon photolysis of H_2 (dmpe = 1,2-bis(dimethylphosphino)ethane) in pentane.[2] In contrast, CO dissociates when $Fe(CO)_5$ is photolyzed, but the iron does not insert into alkane C–H bonds. Matrix isolation studies indicate that at best a weak σ complex is formed between $Fe(CO)_4$ and methane.[3,4] A comparison of $Fe(CO)_4$ and $Fe(dmpe)_2$ chemistry suggests that the metal–alkane interaction increases as CO's are progressively replaced by phosphines and, consequently, as the metal center becomes more electron rich. Little is known about the energetics of these complexes. Luo and Nolan recently reported the enthalpies of substitution of the benzylideneacetone group of (benzylideneacetone)iron tricarbonyl with phosphines or other ligands.[5] Their results provide a comparison of relative bond energies of a variety of ligands, but benzylideneacetone is bidentate and is replaced by two identical ligands, so the enthalpies of individual steps are not know. We have begun systematic studies of the thermochemistry of ligand substitution reactions of $Fe(CO)_4PR_3$ (R = Me and Et, **1a** and **1b**, respectively), $Fe(CO)_3(PMe_3)_2$ (**2**), and $Fe(CO)_3(dmpe)$ (**3**) in cyclohexane. We report the enthalpies of the two steps in CO substitution: CO dissociation (ΔH_1) and subsequent PR_3 addition (ΔH_2, Schemes I and II). We also report the kinetics of the phosphine addition (k_2) which is a reaction of a metal species that is weakly coordinated to cyclohexane.

Scheme I

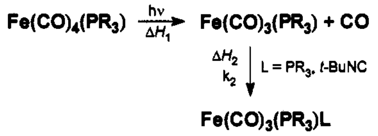

Scheme II

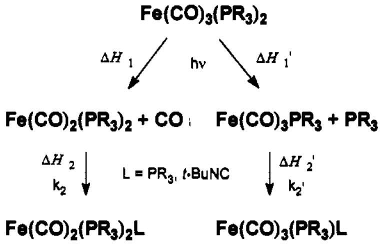

Thermochemical and kinetic measurements were obtained using photoacoustic calorimetry (PAC), but assignments of heats and rates of individual steps requires detailed knowledge of the photochemistry of the complexes under study. This necessitates the measurement of quantum yields (Φ) for ligand substitution. Few quantum yields of iron carbonyl complexes are available,[6–8] and we have recently shown in a communication,[9] in agreement

---

[1] (a) Martinho Simoes, J. A.; Beachamp, J. L. *Chem. Rev.* **1990,** *90,* 629. (b) *Catalysis Looks to the Future;* National Research Council Board on Chemical Sciences and Technology; National Academy Press: Washington, DC, 1992; p 53.

[2] (a) Field, L. D.; George, A. V.; Messerle, B. A. *J. Chem. Soc., Chem. Commun.* **1991,** 1339. (b) Baker, M.V.; Field, L. D. *J. Am. Chem. Soc.* **1987,** *109,* 2825.

[3] Poliakoff, M.; Weitz, E. *Acc. Chem. Res.* **1987,** *20,* 408.

[4] Poliakoff, M.; Turner, J. J. *J. Chem. Soc., Dalton Trans.* **1974,** 2276. Poliakoff, M. *Chem. Soc. Rev.* **1978,** *7,* 527.

[5] (a) Luo, L.; Nolan, S. P. *Organometallics* **1992,** *11,* 3483. (b) (a) Luo, L.; Nolan, S. P. In press.

[6] Warburg, O.; Neglein, E. *Biochem. Z.* **1929,** *204,* 495.

[7] Jaenicke, O.; Kerber, R. C.; Kirsch, P.; Koerner Von Gustorf, E. A.; Rumin, R. *J. Organomet. Chem.* **1980,** *187,* 361.

[8] Angermund, H.; Bandyopadhyay, A. K.; Grevels, F.-W.; Mark, F. *J. Am. Chem. Soc.* **1989,** *111,* 4656.

0002-7863/93/1515-6391$04.00/0

with other studies,[8,10] that the photosubstitution of $Fe(CO)_5$ in solution is distinctly different from that of other metal carbonyls. Most notably, two CO's are substituted in a single-photon process for some nucleophiles but not for others, and for phosphines, the quantum yields vary with the structure of the phosphine. Detailed PAC studies of $Fe(CO)_5$ have been hindered due to the complexity of the photochemistry, while the phosphine derivatives of $Fe(CO)_5$ have proven to be far more tractable. In this paper, we report for the first time the quantum yields for the photosubstitution of **1a**, **1b**, $Fe(CO)_4P(n\text{-}Bu)_3$ (**1c**), **2**, and **3** in the presence of PR_3.

Experimental Section

Materials. All reagents were obtained from Aldrich unless otherwise noted. Immediately before use, solvents (HPLC grade) were refluxed overnight with potassium under argon atmosphere and distilled, and $Fe(CO)_5$ (Strem) was vacuum distilled, trap-to-trap, in subdued light. Phosphines were stored under argon and, unless otherwise described, were used without further purification. Fulgide was obtained from Aberchromics (Cardiff), and potassium ferrioxalate was prepared according to a literature procedure.[11]

Iron carbonyl phosphines were synthesized by photolysis of iron complexes with phosphines in cyclohexane solutions. The solutions were continuously purged with argon in a quartz immersion-well reactor during irradiation with a high-pressure 200-W xenon lamp. In a typical experiment, $Fe(CO)_4PMe_3$ and $Fe(CO)_3(PMe_3)_2$ were synthesized simultaneously by the photolysis of 30 mmol (4 mL) of $Fe(CO)_5$ and 30 mmol (3.1 mL) of trimethylphosphine in 250 mL of hexane. Aliquots were withdrawn periodically for IR analysis, and the photolysis was stopped when the IR bands of products reached a maximum. The solvent and starting materials were removed under vacuum, and from a solid residue, $Fe(CO)_4PMe_3$ and $Fe(CO)_3(PMe_3)_2$ were sublimed at 15 (off-white crystals) and 40 °C (light yellow crystals), respectively. $Fe(CO)_4PEt_3$ and $Fe(CO)_3(PEt_3)_2$ were synthesized using the same method, and $Fe(CO)_4PBu_3$ and $Fe(CO)_3(dmpe)$ were synthesized by reported procedures.[12,13] $Fe(CO)_3(PBu_3)_2$, $Fe(CO)_2(PMe_3)_3$, $Fe(CO)_2(dmpe)(PMe_3)$, and $(t\text{-}BuNC)Fe(CO)_4$ were synthesized by the photolysis of $Fe(CO)_4PBu_3$ with PBu_3, $Fe(CO)_3(PMe_3)_2$ with PMe_3, $Fe(CO)_3(dmpe)$ with PMe_3, and $Fe(CO)_5$ with *t*-BuNC, respectively. $Fe(CO)_3(dmpe)$ was purified by chromatography.[13] All other complexes were purified either by vacuum sublimation or by recrystallization from hexane.

The complexes were characterized by IR and NMR (^1H and ^{13}C) spectroscopies, and the spectra were in good agreement with those previously reported.[13-15] Infrared carbonyl stretching frequencies and carbonyl ^{13}C NMR chemical shifts are reported in the supplementary material. All IR and NMR spectra were obtained on Mattson Galaxy or Polaris FTIR and Varian VXR 300 spectrometers. UV–vis absorbance measurements were determined with the use of a Guilford Response II spectrophotometer.

Photosubstitution Experiments with Dispersed Isonitrile or Carbon Monoxide. To determine if phosphine substitution occurred in addition to CO substitution, iron carbonyl phosphine complexes were irradiated in the presence of *t*-BuNC or CO. For example, an argon-saturated cyclohexane solution of **1b** (4.6 mM) and *t*-BuNC (10 mM) was irradiated 10–20 min at 337 nm in an NaCl IR cell. As an example of an experiment for substitution with CO, a solution of **2** (6 mM) in cyclohexane was bubbled with CO for at least 15 min prior to transfer to an IR cell and subsequent irradiation. Samples were prepared and transferred in an N_2-atmosphere glovebag, and IR spectra were recorded before and after irradiation.

Table I. The Quantum Yield of Photosubstitution of Various Iron Carbonyl Phosphine Complexes at 337 nm

complex (mM)	ligand (mM)	product	Φ^b
1a (8–10)	PMe_3 (50–150)	$Fe(CO)_3(PMe_3)_2$	0.56(3)
1b (7–9)	PEt_3 (41–150)	$Fe(CO)_3(PEt_3)_2$	0.54(2)
1c (8)	PBu_3 (70–150)	$Fe(CO)_3(PBu_3)_2$	0.62(1)
2 (8–10)	PMe_3 (13–50)	$Fe(CO)_2(PMe_3)_3$	0.50(3)
2 (8–10)	CO^a	$Fe(CO)_4PMe_3$	0.030(1)
3 (5–9)	PMe_3 (50–100)	$Fe(CO)_2(dmpe)(PMe_3)$	0.47(3)

[a] Saturated in cyclohexane; see text. [b] Parenthetical values are the errors in the last digit(s).

Quantum Yield Determinations. All solutions were prepared under argon and transferred using cannula techniques. Iron complexes were weighed in a 10 mL volumetric flask, which was sealed with a septum, evacuated to a pressure of less than 100 μm of Hg, and filled with argon. A stock solution of a ligand in cyclohexane was then transferred to the flask. The resulting solution was bubbled with argon or CO for 15–20 min. The concentrations of the complexes and phosphines are listed in Table I. A 2-mL sample solution of phosphine and iron complex (actual volume determined gravimetrically) was irradiated in a 1-cm path length septum-sealed quartz cuvette (Wilmad No. 110CQ) with a high-pressure 150-W xenon lamp (PTI lamp housing and power supply Models A1010 and LPS-220, respectively). The light was filtered with a 10-cm water filter, a Schott filter (UG5), a neutral density filter, and a 337-nm interference filter (10 nm fwhm, Corion P10F). The beam cross-section at the cuvette was about 0.5 cm^2. The sample was kept at 25 ± 0.1 °C. Part of the light was focused on a photodiode to monitor any fluctuation in the light intensity during the irradiation. To ensure accuracy, the light intensity was determined with several chemical actinometers (fulgide, ferrioxalate, azobenzene, and dimethylanthracene).[11,16] The irradiation was typically $3\text{–}12 \times 10^{-10}$ einstein s^{-1} for 5 to 20 min. The extent of photoproduct formation was determined using FTIR spectroscopy. The spectrometer was calibrated with authentic samples of the photoproducts using the Mattson PLS-Quant software. The initial absorbance of the sample solutions at 337 nm was always greater than 3. The conversion was kept below 10% to avoid secondary photolysis, and corrections for the inner-filter effect were made only in those cases mentioned. In most of the cases the molar absorptivity of the photoproducts was less than or equal to the molar absorptivity of the starting complex. The quantum yields (Φ) were independent of the light intensity, ligand concentration (for at least a 5-fold change), irradiation time, and conversion (1–10%) of the starting complex. Reported quantum yields are the average of five measurements from two independent experiments. The luminescence for 337-nm excitation was determined with a Perkin-Elmer MPF-3 spectrofluorimeter and was found to be negligible for each compound.

Photoacoustic Calorimetry Experiments. The instrumentation and theory of photoacoustic calorimetry (PAC) have been described before.[17,18] Briefly, a nanosecond light pulse from a nitrogen laser (337.1 nm) is weakly focused on a metal complex solution in a flow cell (Figure 1). The absorbed light initiates chemical and physical processes that deposit heat. Thermal expansion produces a pressure (acoustic) wave that can be detected with an ultrasonic transducer (Panametrics V103). The transducer signal is amplified and captured on a digital oscilloscope (Tektronix 2430). The amplitude and phase of the transducer signal are dependent on the amount and rate of heat deposition after the laser pulse, as well as on the frequency response of the transducer. Deconvolution of a signal with the response function of the instrument provides thermodynamic and kinetic data about the reactions initiated by photolysis.

(a) Sample Preparation and Delivery. In a typical experiment, 12.5 mg (51 μmol) of **1a** and 65 mg (0.35 mmol) of ferrocene were weighed in separate 25 mL volumetric flasks. Further manipulations of **1a** were carried out in septum-sealed glassware. The flask containing **1a** was evacuated and filled with argon or helium. Both flasks were filled to the mark with cyclohexane. Three graduated reservoirs, one each for the **1a**

---

(9) Nayak, S. K.; Burkey, T. J. *Inorg. Chem.* **1992**, *31*, 1125.

(10) Schroeder, M. A.; Wrighton, M. S. *J. Am. Chem. Soc.* **1976**, *98*, 551.

(11) Hatchard, C. G.; Parker, C. A. *Proc. R. Soc. (London)* **1953**, *A220*, 104.

(12) Albers, M. O.; Coville, N. J. *J. Organomet. Chem.* **1981**, *217*, 385.

(13) Akhtar, M.; Elles, P. D.; MacDiarmid, A. D.; Odom, J. D. *Inorg. Chem.* **1972**, *11*, 2917.

(14) (a) Van Rentergem, M.; Van Der Kelen, G. P.; Claeys, E. C. *J. Mol. Struct.* **1982**, *80*, 317. (b) Reckziel, A.; Bigorgne, M. *J. Organomet. Chem.* **1965**, *3*, 341. (c) Conder, H. L.; Darensbourg, M. Y. *J. Organomet. Chem.* 1974, *67*, 93. (d) Karsch, H. H.; Friedrich, H. F.; Schmidbaur, H. *Chem. Ber.* **1977**, *110*, 2200.

(15) (a) Mann, B. E. *Adv. Organomet. Chem.* **1974**, *67*, 93. (b) Mann, B. E. *J. Chem. Soc., Chem. Commun.* **1971**, 1173. (c) Whitmire, K. N.; Lee, T. R. *J. Organomet. Chem.* **1985**, *282*, 95.

(16) (a) Heller, H. G.; Langan, G. R. *J. Chem. Soc., Perkin Trans. II* **1981**, 341. (b) Adick, H. J.; Schmidt, R.; Brauer, H. D. *J. Photochem. Photobiol. A* **1988**, *45*, 89. (c) Gauglitz, G.; Hubig, S. *J. Photochem.* **1981**, *15*, 255.

(17) (a) Burkey, T. J. In *Energetics of Organometallic Species*; Martinho Simoes, J. A., Ed.; Nato ASI Series C, No. 367; Kluwer: Dordrecht, 1992; pp 75–94. (b) Burkey, T. J.; Majewski, M.; Griller, D. *J. Am. Chem. Soc.* **1986**, *108*, 2218. (c) Burkey, T. J. *Polyhedron* **1989**, *8*, 2681. (d) Burkey, T. J. *J. Am. Chem. Soc.* **1990**, *112*, 8239. (e) Morse, J., Jr.; Parker, G.; Burkey, T. J. *Organometallics* **1989**, *8*, 2471.

(18) Braslavsky, S. E.; Heibel, G. E. *Chem. Rev.* **1992**, *92*, 1381.

(19) Rudzki Small, J.; Libertini, L. J.; Small, E. W. *Biophys. Chem.* **1992**, *42*, 29.

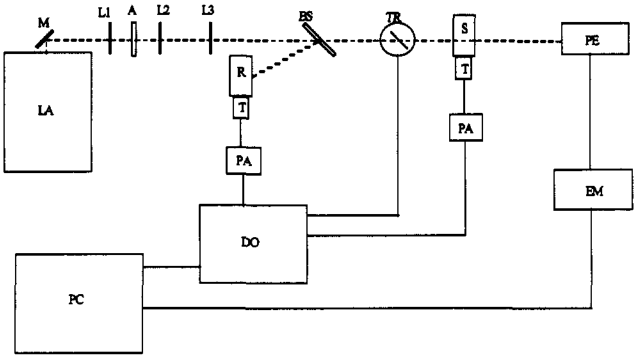

Figure 1. Diagram of PAC apparatus: LA = nitrogen laser, PE = pyroelectric probe, EM = energy meter, DO = digital oscilloscope, R = reference cuvette, S = sample cell, BS = beam splitter, T = transducer, PA = preamplifier, TR = trigger, L1 and L2 = biconvex lenses of 10 cm focal length, L3 = lens of 25 cm focal length, A = adjustable aperture, and M = mirror.

solution, a reference solution (ferrocene), and neat cyclohexane, were connected to the sample flow cell via a glass manifold with Teflon stopcocks. The manifold and reservoirs were oven dried at 125 °C, assembled hot, and purged with helium. A ferrocene solution (10 mL) was pipetted to a reservoir and diluted with cyclohexane to about 100 mL to obtain an absorbance of about 0.1 at 337 nm. The solution of **1a** (16 mL) was transferred with a cannula to a septum-sealed reservoir and likewise diluted. Freshly distilled trimethylphosphine (30 μL, 2.8 mmol) was transferred to the reservoirs with a microsyringe. The final concentrations of **1a** and **1b** were 3×10^{-4} M and those of **2** and **3** were 1.2×10^{-4} M.

The laser pulse rate was 1 Hz, and about 25 μJ per pulse reached the probe when the flow cell contained cyclohexane. To ensure fresh solution was provided for each laser pulse the solution flow rate was increased until the amplitude of the transducer signal was independent of the flow rate.

(b) Data Acquisition and Processing. The transducer signals from the sample and reference cells were digitized for each laser shot (1024 points at 10-ns intervals). Data acquisition and processing were facilitated by AQPAC, a computer program developed by Bruce Campbell in our lab. This program transfers data shot by shot from the oscilloscope and the energy meter to the computer. Shots with energy 5–10% outside the average shot energy were not transferred. For each measurement, data for at least 32 shots were acquired, corrected for baseline drift, and averaged. The data for a reference solution in the sample cell were acquired before and after acquiring data for a solution of an iron phosphine complex. This was necessary to minimize the effects of instrument drift. Generally, 3 to 4 measurements were made for each ligand concentration. Data for solvent were collected before and after each series of measurements. To correct for fluctuations of laser pulse energies, energy meter measurements (E) were normalized by dividing them by the signal amplitude of the reference cell transducer. The reference cell contained a ferrocene solution. A normalized signal for the measurement of a solution in the flow cell (S_n) is obtained with the use of eq 1 where S is the averaged observed signal, R is the averaged amplitude of the signal

$$S_n = SE_0/R(E_0 - E) \tag{1}$$

from the reference cell transducer, E is the normalized energy meter measurement for a reference or sample solution, and similarly E_0 is for neat cyclohexane. Therefore, S_n is adjusted for variations in light absorbance and laser pulse energies.

A normalized signal for a sample solution was deconvoluted with a normalized signal for a reference solution using the MQ program which has been thoroughly tested.[19] The excited state of ferrocene in the reference solution decays non-radiatively in less than a nanosecond with a quantum yield of 1.00.[20] Thus the decay of the ferrocene excited state is much shorter than the response time of our transducer, and the observed signal provides a response function for the PAC apparatus. Furthermore, the amount of heat deposited by ferrocene is known precisely since it corresponds to the energy of the photons absorbed. The program provides the magnitudes of the sample heat decays expressed as a fraction of the energy deposited by a reference solution (ϕ) as well as the lifetimes of the sample heat decays (τ). One or more heat decays may be detected. The first heat decay is always due to processes evolving with lifetimes much shorter than the response time of the transducer ($<10^{-7}$ s), and the signal is not distinguishable from that of the instrument response function. Hence the magnitude of the first heat decay (ϕ_1) but not the lifetime can be determined. A second heat decay, due to processes evolving with lifetimes near the response time of the transducer, can be detected (10^{-7}–10^{-5} s). Both the magnitude (ϕ_2) and the lifetime (τ_2) of the second heat decay can be determined. The ϕ_1, ϕ_2, and τ_2 values were optimized to obtain the lowest χ^2 value[19] which was less than 5×10^{-5}.

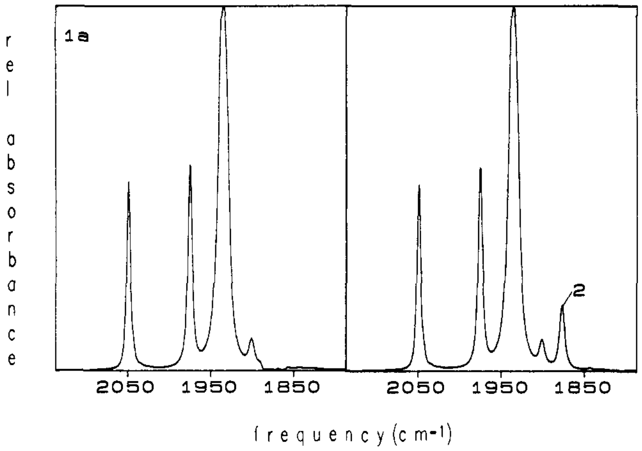

Figure 2. Infrared spectra in the CO stretching region of **1a** with PMe_3 in cyclohexane before (left) and after (right) 337-nm irradiation.

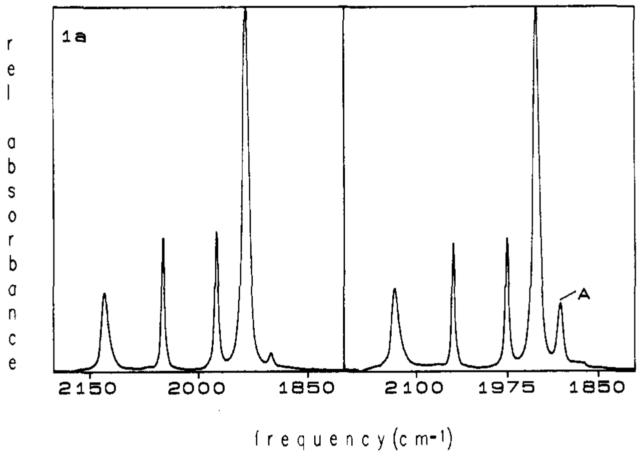

Figure 3. Infrared spectra in the CO stretching region of **1a** with $CNC(CH_3)_3$ in cyclohexane before (left) and after (right) 337-nm irradiation. Peak A is due to $Fe(CO)_3(CNC(CH_3)_3)(PMe_3)$.

Results

Photosubstitution and Actinometry. Photolysis of **1a–c** in cyclohexane results in the substitution of CO but not phosphine. Figure 2 shows the IR spectrum in the CO stretching region of **1a** in the presence of PMe_3 before and after irradiation; only a single band, at 1876 cm^{-1}, appears. This band is assigned to **2** by comparison with literature values and with a spectrum of pure **2** in cyclohexane. While this indicates that CO dissociates upon photolysis it does not rule out the possibility that PMe_3 also dissociates. The latter process would be undetected since the dispersed ligand is also PMe_3 and addition simply reforms **1a**. The IR spectrum of an irradiated cyclohexane solution of **1a** and *t*-BuNC reveals that CO undergoes substitution upon irradiation but not PMe_3: only a single band at 1902 cm^{-1} appears (Figure 3). The 1902-cm^{-1} band increases with irradiation time and does not appear in the absence of **1a** or *t*-BuNC. Assignment of the band to *trans*-$Fe(CO)_3(PMe_3)$(*t*-BuNC) is consistent with the intermediate position of 1902 cm^{-1} between the bands due to *trans*-$Fe(CO)_3(PMe_3)_2$ (1876 cm^{-1}) and *trans*-$Fe(CO)_3$(*t*-

---

[20] Maciejewski, A.; Jaworska-Augustyniak, A.; Szeluga, Z.; Wojtczak, J.; Karolczak, J. *Chem. Phys. Lett.* **1988** *153*, 227.

BuNC)$_2$ (1927 cm^{-1}).[14b,21] No bands at 1960, 1989, and 2060 cm^{-1} due to Fe(CO)$_4$(*t*-BuNC), the expected product of PMe$_3$ substitution, were observed.[21] Similarly, only a single new band at 1902 cm^{-1} was observed when **1b** was irradiated in the presence of *t*-BuNC. These results indicate that Fe(CO)$_4$PR$_3$ complexes substitute CO but not PR$_3$ upon irradiation. In all cases, the irradiated solution had only one new band consistent with the formation of only one product. Quantum yields range from 0.54 to 0.62 for formation of Fe(CO)$_3$(PR$_3$)$_2$ from **1** and PR$_3$ (R = Me, Et, and *n*-Bu) and are reported in Table I.

Irradiation experiments with **2** indicate that both CO and PMe$_3$ photosubstitute. Upon irradiation of **2** with PMe$_3$, a CO substitution product, Fe(CO)$_2$(PMe$_3$)$_3$, is formed in high yield. The product bands at 1828 and 1888 cm^{-1} were the only ones that appeared and were identified by a comparison with a spectrum of pure Fe(CO)$_2$(PMe$_3$)$_3$ and literature values.[14d] Irradiation of **2** with *t*-BuNC in cyclohexane results in two new bands at 1902 and 1851 cm^{-1}. The formation of Fe(CO)$_2$(PMe$_3$)$_2$(*t*-BuNC) in high yield by CO substitution is consistent with its assignment to the larger band at 1851 cm^{-1}. The smaller band at 1902 cm^{-1} is due to Fe(CO)$_3$(PMe$_3$)(*t*-BuNC) (*vide supra*), and its formation is consistent with the dissociation of PMe$_3$ upon photolysis of **2**. Photosubstitution of coordinated phosphine was further confirmed by irradiating a 6 mM solution of **2** in CO-saturated cyclohexane; the only new bands to appear in the IR spectra of the solution were at 1937, 1979, and 2050 cm^{-1} due to **1**.[14b,c]

The quantum yield for formation of **1** from **2** was 0.03 in CO-saturated cyclohexane (10 mM)[22] but only 0.02 in solutions having half the CO-saturated concentration. In the latter experiments, bands at 1920 and 1988 cm^{-1} are observed in addition to those observed for **1**. The additional bands are probably due to the products arising from the reaction of intermediates with **2**. The quantum yield of 0.03 for **2** in CO-saturated solutions thus should be considered a lower limit since it is uncertain whether the intermediate is completely scavenged by CO. Nevertheless, the absence of any other bands in these experiments indicates that all Fe(CO)$_3$PMe$_3$ was scavenged by the added CO, and we believe that the quantum yield in the CO-saturated solutions of **2** should be close to the limiting value.

Photolysis experiments with **3** indicate CO but no phosphine substitution. The IR spectrum of **3** and PMe$_3$ in cyclohexane after irradiation revealed new bands only at 1840 and 1895 cm^{-1} which, by analogy to Fe(CO)$_2$(PMe$_3$)$_3$, were assigned to Fe(CO)$_2$(dmpe)PMe$_3$. No IR band for Fe(CO)$_3$(η^1-dmpe)(PMe$_3$), a dmpe substitution product, was observed. This product should have an IR band similar to that of Fe(CO)$_3$(PMe$_3$)$_2$ (1875 cm^{-1}) and different from that of the parent complex (1903, 1917, and 1988 cm^{-1}).[13,23] The quantum yields for PMe$_3$ and CO substitution of **2** and for CO substitution of **3** are corrected for the inner-filter effect and are reported in Table I.[24] The corrections are necessary because the molar absorptivity of the photoproducts (Fe(CO)$_2$(PMe$_3$)$_3$, ϵ = 1960 M^{-1} cm^{-1}; Fe(CO)$_2$(dmpe)PMe$_3$, ϵ = 1600 M^{-1} cm^{-1}) at 337 nm is much larger than that of the starting complexes (**2**, ϵ = 350 M^{-1} cm^{-1}; **3**, ϵ = 860 M^{-1} cm^{-1}).

Photoacoustic Calorimetry. For photolysis of **1–3**, two heat decays were detected in the presence of dispersed ligand. The magnitudes of the first heat decays (ϕ_1) were independent of ligand concentration (*vide infra*) and were the same as when no ligand was added. The first heat decays produced no signal shift relative to the reference signal so the rates of decay must be in excess of 10^7 s^{-1}. The second heat decays (ϕ_2) had decay rates ($1/\tau_2$) that increased linearly with ligand concentration and must be in the range of 10^7–10^5 s^{-1} since a signal shift was detectable. When ligand was present, no improvement in the signal fit was observed when modeled with 1 or 3 heat decays. We assign ϕ_1 to CO dissociation and subsequent coordination of solvent (and nonproductive processes, *vide infra*) and the second heat decay ϕ_2 to displacement of solvent by dispersed ligand (Schemes I and II). These assignments are consistent with the results of previous studies where the photodissociation of CO from related complexes is known to occur on a subnanosecond time scale, and the reaction of solvent-coordinated metal centers with dispersed ligand occurs on a nano- to microsecond time scale.[25,26] The heat decays and lifetimes determined for each complex at various ligand concentrations are presented in the supplementary material. In the case of Fe(CO)$_4$PMe$_3$, the ϕ_1 was slightly dependent on ligand concentration, and the value reported is the measurement for zero ligand concentration.

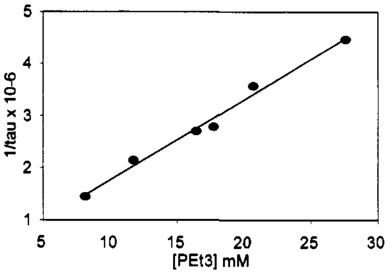

Figure 4. Plot of $1/\tau_2$ vs PEt$_3$ concentration for reactions taking place after the photolysis of **1b**.

The heat deposited by reactions associated with the first and second heat decays (ΔH_1 and ΔH_2, respectively) was calculated from the following equations where Φ is the quantum yield for

$$\Delta H_1 = E_{h\nu}(1 - \phi_1)/\Phi \tag{2}$$

$$\Delta H_2 = -E_{h\nu}\phi_2/\Phi \tag{3}$$

$$1/\tau_2 = k_0 + k_2[\mathrm{L}] \tag{4}$$

the photosubstitution of the iron phosphine carbonyl and [L] is the ligand concentration (see Schemes I and II).[27] Note that eq 3 differs from eq 2 since the latter includes a correction for that heat deposited by photons that do not initiate a chemical reaction. The second-order rate constants (k_2) for phosphine addition were obtained from the slopes of plots of $1/\tau_2$ vs ligand concentration (eq 4, Figure 4). In the case of **2** where PMe$_3$ also photodissociates, the value of ΔH_1 was corrected for the contribution of $\Delta H_1'$ (Scheme II) using eq 5. The $\Delta H_1'$ is equal to $-\Delta H_2$ for **1a** and

$$\Delta H_1 = [E_{h\nu}(1 - \phi_1) - \Phi'\Delta H_1']/\Phi \tag{5}$$

Φ' is reported in Table I. The values for ΔH_2 and k_2 are not as easily corrected. The amplitude of the observed second heat decay, $\phi_{2+2'}$, does not necessarily equal the sum of ϕ_2 (PMe$_3$ addition to Fe(CO)$_2$(PMe$_3$)$_2$) and $\phi_{2'}$ (PMe$_3$ addition to Fe(CO)$_3$(PMe$_3$)) because k_2' may not be equal to k_2 (experimental results: $\phi_{2+2'}$

---

(21) (a) Cotton, F. A.; Parish, R. V. *J. Chem. Soc.* **1960**, 1440. (b) Albers, M. O.; Coville, N. J.; Singleton, E. *J. Chem. Soc., Dalton Trans.* **1982**, 1069.

(22) Wilhelm, E.; Battino, R. *Chem. Rev.* **1973**, *73*, 1.

(23) Note that η^1-DMPE and PMe$_3$ should have a similar effects on the CO stretching frequency since Fe(CO)$_4$PPh$_3$ and Fe(CO)$_4$(η^1-DPPE) (DPPE = bis(diphenylphosphino)ethane) have very similar IR spectra in the CO stretching region: see ref 14.

(24) Nasielski, J.; Colas, A. *Inorg. Chem.* **1978**, *17*, 237.

(25) (a) Simon, J. D.; Xie, X. *J. Phys. Chem.* **1989**, *93*, 291. (b) Wang, L.; Zhu, X.; Spears, K. G. *J. Am. Chem. Soc.* **1988**, *110*, 8695. (c) Joly, A. G.; Nelson, K. A. *J. Phys. Chem.* **1989**, *93*, 2876. (d) Simon, J. D.; Xie, X. *J. Phys. Chem.* **1987**, *91*, 5538. (e) Lee, M.; Harris, C. B. *J. Am. Chem. Soc.* **1989**, *111*, 8963. (f) Yu, S.-C.; Xu, X.; Lingle, R., Jr.; Hopkins, J. B. *J. Am. Chem. Soc.* **1990**, *112*, 3668. (g) Simon, J. D.; Xie, X. *J. Phys. Chem.* **1986**, *90*, 6751.

(26) (a) Dobson, G. R.; Asali, K. J.; Cate, C. D.; Cate, C. W. *Inorg. Chem.* **1991**, *30*, 4471. (b) Zhang, S.; Zang, V.; Bajaj, H. C.; Dobson, G. R.; van Eldik, R. *J. Organomet. Chem.* **1990**, *397*, 279. (c) Zhang, S.; Dobson, G. R. *Inorg. Chim. Acta* **1989**, *165*, 11.

(27) (a) Yang, G. K.; Vaida, V.; Peters, K. S. *Polyhedron* **1988**, *7*, 1619. (b) Rudzki, J.; Goodman, J. L.; Peters, K. S. *J. Am. Chem. Soc.* **1985**, *107*, 7849.

Table II. PAC Data for the Substitution of Iron Carbonyl Phosphine Complexes

complex	ligand (mM)	ϕ_1	ϕ_2	ΔH_1	ΔH_2, kcal/mol	$10^{-8}k_2$, M^{-1} s^{-1}
1a	PMe_3 (0–9)	0.73(1)[a]	0.27(2)	40.9(26)	–40.9(30)	7.0(10)
1a	PEt_3 (2–15)	0.75(1)	0.26(1)	37.9(20)	–39.4(26)	3.9(5)
1b	PEt_3 (6–27)	0.75(1)	0.28(1)	39.2(20)	–45.5(20)	1.5(2)
2	PMe_3 (2–14)	0.81(1)	0.115(10)	29.8(26)	–19.5(10)	3.7(2)
3	PMe_3 (1–7)	0.80(1)	0.18(1)	36.1(26)	–32.5(30)	5.7(15)

[a] Parenthetical values for ϕ_1, ϕ_2, ΔH_1, ΔH_2, and k_2 are the errors in the last digit(s); errors include errors propagated from ϕ and Φ and are reported as σ.

= 0.13(1) and $k_{2+2'} = 4.0(1) \times 10^8$ M^{-1} s^{-1}). Since ϕ_2' and τ_2' can be determined from $\Delta H_2'$ and k_2' (which are equal to the ΔH_2 and k_2 for **1a**, respectively) a waveform resulting from $\Delta H_2'$ can be calculated by convolution of the heat decay for $\Delta H_2'$ with the reference signal. Likewise, simulated signals for ΔH_2 were generated by using various ϕ and τ and were added to the waveform for $\Delta H_2'$. From several trials, the resultant signal that best fit the experimental signal was determined (calculated: $\phi_{2+2'} = 0.13$ and $k_{2+2'} = 4.0 \times 10^8$ M^{-1} s^{-1}). The corrections for the PMe_3 dissociation and recombination pathway make ΔH_1 about 3 kcal/mol more exothermic and ΔH_2 about 3 kcal/mol more endothermic. The corrected values for **2** are reported with the PAC results for the other complexes in Table II.

If there is photolytic chelate ring opening of **3**, our results indicate that it is followed by ring closure on a time scale faster than our instrument response. Such a process would be thermoneutral and therefore is another pathway where the total energy of a photon is deposited as heat. Our quantum yield experiments demonstrated that the ring closure (eq 6, path a) must be much faster than reaction with 50 mM PMe_3 (eq 6, path b) since only

$$Fe(CO)_3(dmpe) \xleftarrow{a} Fe(CO)_3(\eta^1\text{-dmpe}) \xrightarrow[+PMe_3]{b} Fe(CO)_3(\eta^1\text{-dmpe})(PMe_3) \quad (6)$$

CO substitution product was observed. An estimated pseudo-first-order rate constant of 3.5×10^7 s^{-1} for path b can be made using the second-order rate constant for PMe_3 addition to $Fe(CO)_3PMe_3$ (Table II). Experimentally, we find this rate is about 3 times faster than can be resolved by our instrument. Therefore the heat of chelate ring opening and closure contributes only to ϕ_1, and it would be included with the heat of other processes that lead to no net reaction and need not be considered individually.

Discussion

Quantum Yields of Substitution. For iron tetracarbonyl phosphines, the quantum yields range from 0.54 to 0.62 at 337 nm. For comparison, the quantum yield at 302 nm for the photosubstitution of ((*E*)-cyclooctene)$Fe(CO)_4$ with (*E*)-cyclooctene is 0.59 ± 0.04.[8] Thus the quantum yield for CO photosubstitution on ((*E*)-cyclooctene)$Fe(CO)_4$ is essentially the same as that on $Fe(CO)_4PR_3$, indicating that the quantum yields show little dependence on the uniquely coordinated ligand or the incoming ligand (for these ligands at least).

Angermund *et al.* suggested cyclooctene dissociation may also occur in competition with CO dissociation and could account for a quantum yield of less than unity.[8] In their studies the dispersed and coordinated olefins were identical, and the dissociated olefin would be replaced by an olefin of the same structure. (Thus, no olefin substitution would be observed in their experiments if the olefin were to dissociate, making it impossible to measure directly L photosubstitution or photodissociation on $Fe(CO)_4L$ complexes.) Our studies of $Fe(CO)_4PR_3$ suggest that olefin dissociation may not occur. The similarity in quantum yields for photosubstitution of monophosphine and monoolefin complexes indicates that the photosubstitution mechanisms are similar. We observed no $Fe(CO)_5$ formation upon photolysis of $Fe(CO)_4PR_3$ in the presence of CO and no $Fe(CO)_4$(*t*-BuNC) formation in the presence of *t*-BuNC; hence, PR_3 photosubstitution on $Fe(CO)_4PR_3$ can be ruled out. More specifically either the phosphine does not dissociate upon photolysis or it does not escape the solvent cage before recombination with $Fe(CO)_4$. Considering the similar photochemistry, we suspect that olefin substitution does not occur upon photolysis from ((*E*)-cyclooctene)$Fe(CO)_4$.

In contrast, phosphine photosubstitution does occur with $Fe(CO)_3(PMe_3)_2$ albeit the yield is low. These results are consistent with previous studies where phosphine and phosphite photosubstitution were observed for $Fe(CO)_3[P(p\text{-}C_6H_4CH_3)_3]_2$ and $Fe(CO)_3(POEt_3)_2$, respectively.[28,29] We find that phosphine substitution is non-existent in the case of a bidentate phosphine, *e.g.*, $Fe(CO)_3$(dmpe). It is likely that Fe–P dissociation still occurs in this case but ring closure is much faster than reaction with dispersed ligand. Our results are in agreement with recent photoacoustic calorimetry studies of $CpMn(CO)_2(\eta^1\text{-dmpe})$ that demonstrated that upon photodissociation of CO, chelate ring closure occurred with a rate faster than 100 ns.[30]

For all complexes studied, the dispersed phosphine concentration was in large excess of the iron complex concentration, and the substitution quantum yields were independent of the phosphine concentration. We conclude that the intermediate formed upon CO dissociation is completely scavenged by phosphine and that the quantum yield of CO substitution is equal to the quantum yield for CO dissociation.

Kinetics and Thermochemistry. The rate constants for phosphine addition show a small but significant dependence on steric effects. $Fe(CO)_3PMe_3$ reacts with PMe_3 1.8 times faster than with the bulkier PEt_3, and PEt_3 reacts with $Fe(CO)_3PMe_3$ 2.5 times faster than with $Fe(CO)_3PEt_3$ where the coordinated phosphine is larger. These data indicate the steric bulk of both the attacking and coordinated phosphine affects the rate of phosphine attack on the iron center. The other kinetic data are likewise explained by steric effects. PMe_3 reacts with $Fe(CO)_2(PMe_3)_2$ 1.8 times slower than with $Fe(CO)_3PMe_3$ since the former has two phosphine groups. The PMe_3 reaction with $Fe(CO)_2(PMe_3)_2$ is slower than with $Fe(CO)_2$(dmpe) since the dmpe group is less bulky than two PMe_3 groups.

Various facts suggest that the Fe–cyclohexane interaction is substantially weaker than that observed for Cr, Mo, or W.[17] The rate constants for phosphine addition for the Fe complexes are large and some are within an order of magnitude of the diffusion-controlled limit. So if the solvent is coordinated, it must be a fairly weak interaction. The rate of alkane displacement on $Cr(CO)_5$(alkane) is typically an order of magnitude slower than those of the Fe complexes.[26,27,31] For example, the rate constant for displacement of heptane by N(*n*-Bu)$_3$ is 1.2×10^7 M^{-1} s^{-1}.[27] Kinetic and matrix isolation studies indicate the interaction between $Ru(dmpe)_2$ and an alkane is negligible and the rate of

---

(28) Black, J. D.; Boylan, M. J.; Braterman, P. S.; Wallace, W. J. *J. Organomet. Chem.* **1973**, *63*, C21.

(29) Knorr, M.; Schubert, U. *J. Organomet. Chem.* **1989**, *365*, 151.

(30) Hester, D. M.; Sun, J.; Harper, A. W.; Yang, G. K. *J. Am. Chem. Soc.* **1992**, *114*, 5234.

(31) (a) Kelly, J. M.; Bent, D. V.; Hermann, H.; Schulte-Frohlinde, D.; Koerner von Gustorf, E. *J. Organometal. Chem.* **1974**, *69*, 259. (b) Kelly, J. M.; Hermann, H.; Koerner von Gustorf, E. *J. Chem. Soc., Chem. Commun.* **1973**, 105. (c) Church, S. P.; Grevels, F.-W.; Hermann, H.; Schaffner, K. *Inorg. Chem.* **1985**, *24*, 418. (d) Hermann, H.; Grevels, F.-W.; Henne, A.; Schaffner, K. *J. Phys. Chem.* **1982**, *86*, 5151.

reaction with PMe_3 in cyclohexane is comparable to the values in Table II (3.8×10^8 M^{-1} s^{-1}).[32] By analogy, the complexes formed by CO dissociation in the current study are expected to bond alkanes very weakly.

Some data are available on the energetics of CO dissociation from iron complexes. In a previous study, the activation enthalpy for the dissociative CO substitution of $Fe(CO)_4(PPh_3)$ with PPh_3 was found to be 42.5 kcal/mol in decalin.[33] Interestingly, this value is within experimental error of our results for CO dissociation for monophosphine complexes. For comparison, the gas-phase bond energy of the $Fe(CO)_4$–CO bond has been reported to be 41.5 kcal/mol.[34] If the $Fe(CO)_3(PPh_3)$–CO bond is completely broken in the transition state (with little solvent coordination) then the activation enthalpy is a good measure of the Fe–CO bond dissociation energy. If there is some Fe–solvent bonding in the transition state, the $Fe(CO)_3(PPh_3)$–CO bond energy will be larger than 42 kcal/mol depending on the extent of solvent coordination in the transition state. Assuming that the enthalpy of non-stereospecific solvation of reactants and intermediates is nearly the same, ΔH_1 will be equal to the difference in enthalpies of the bonds broken and formed, *i.e.*, the Fe–CO and Fe–cyclohexane bonds.[35] Thus, ΔH_1 is a lower limit for the Fe–CO bond energy.

The dissociation of CO becomes less endothermic with more coordinated phosphines (10 kcal/mol difference for **1a** and **2**). Since ΔH_1 is the difference between the Fe–CO and Fe–cyclohexane bonds this means that the Fe–CO bond is becoming weaker and/or the Fe–cyclohexane bond is becoming stronger. It seems unlikely that an intrinsically weak interaction, such as that between these Fe complexes and cyclohexane, can be increased by 10 kcal/mol with a single ancillary ligand substitution. It could be argued that the greater electron density at the metal center will increase backbonding with a C–H antiboding orbital leading to a transition from a σ-complex (two-electron three-center bond) to an alkyl hydride (two localized σ bonds).[36] Yet CO is a better π acid than cyclohexane, and the strength of the Fe–CO bond would be expected to increase as well. Thus, one must postulate the Fe–cyclohexane bond strength would have to increase more than the Fe–CO bond strength. Assuming this were the case then the cyclohexane interaction with $Fe(CO)_2(PMe_3)_2$ would be 10 kcal/mol greater than that with $Fe(CO)_3(PMe_3)$. This may seem reasonable in light of the fact that two more coordinated phosphines provide a reactive metal center (*i.e.* $Fe(PMe_3)_4$) known to cyclometalate and insert into alkane CH bonds;[2,37] nevertheless, a 10-kcal/mol increase in the interaction with cyclohexane is inconsistent with the small changes of k_2 reported in Table II. Furthermore, it is not clear how increasing the electron density at the metal affects the relative strengths of the σ and π bonding interactions; increased electron density at the metal center could make σ-donation less favorable for both CO and cyclohexane. Previous research from our labs has shown that metal–solvent interactions may be minimized in fluorocarbon solvents;[17,38] thus, experiments in these media are being pursued as are theoretical studies to clarify the bonding interactions in both low-valent and high-valent transition-metal complexes.[39]

The enthalpy of CO substitution by PR_3 on **1**–**3** is the sum of the ΔH_1 and ΔH_2. If solvation of reactants and products is similar, the sum of ΔH_1 and ΔH_2 will be equal to the difference in the bond energies formed and broken (*vide supra*). For **1**, the substitution of CO by PR_3 is thermoneutral or somewhat exothermic, indicating that the $Fe(CO)_3(PR_3)$–PR_3 bond is as strong or stronger than the $Fe(CO)_3(PR_3)$–CO bond. For **2** the substitution of CO by PMe_3 is endothermic by 10 kcal/mol, indicating the $Fe(CO)_2(PMe_3)_2$–CO bond is stronger than the $Fe(CO)_2(PMe_3)_2$–PMe_3 bond. So the substitution of CO by PR_3 becomes energetically less favorable when the number of coordinated phosphines increases from one to two. As before, it might be argued that a second phosphine further increases the electron density at the metal center and this strengthens the Fe–CO bond via back-bonding and weakens the Fe–PR_3 bond. Alternatively, the substitutions on **1** and **2** are stereochemically different since an axial CO is replaced by an axial phosphine on **1** and an equatorial CO is replaced by an equatorial phosphine on **2**. Back-bonding may be favored in an equatorial position,[40] so the substitution of an equatorial CO by PR_3 would be less favorable than the substitution of an axial CO by PR_3. Nevertheless, if ΔH_1 is determined primarily by the Fe–CO bond strength, these arguments do not explain the fact that ΔH_1 for **2** is less than it is for **1**. A steric effect is more consistent with the results.

The replacement of CO by PR_3 on **2** occurs at a more congested equatorial position and makes the metal center more crowded. If ΔH_1 and ΔH_2 are determined primarily by the respective Fe–CO and Fe–PR_3 bond strengths then the $Fe(CO)_3(PMe_3)$–CO (**1**) bond is stronger than the $Fe(CO)_2(PMe_3)_2$–CO (**2**) bond and the $Fe(CO)_3(PMe_3)$–PMe_3 (**2**) bond is stronger than the $Fe(CO)_2(PMe_3)_2$–PMe_3 bond. The weaker Fe–CO bond in **2** can be explained by the fact that when CO dissociates there is greater relief of steric repulsion than in **1**. Similarly, greater steric repulsion accompanies PMe_3 addition to $Fe(CO)_2(PMe_3)_2$ than to $Fe(CO)_3(PMe_3)$, the intermediates formed by CO dissociation from **2** and **1**, respectively. Consistent with a steric effect, the magnitude of the difference in the enthalpies for phosphine addition (21 kcal/mol) is greater than the difference for CO dissociation (11 kcal/mol). Likewise, steric effects explain the differences between **2** and **3**; the enthalpy of CO substitution by PMe_3 for **2** (eq 7, $\Delta H_1 + \Delta H_2 = 10$ kcal/mol) is more endothermic than for **3** (eq 8, $\Delta H_1 + \Delta H_2 = 3.6$ kcal/mol). The dmpe ligand which is constrained to cis positions (equatorial and axial) is sterically less demanding on the metal center than two PMe_3 in trans positions (axial).

$$Fe(CO)_3(PMe_3)_2 + PMe_3 \rightarrow Fe(CO)_2(PMe_3)_3 + CO \quad (7)$$

$$Fe(CO)_3(dmpe) + PMe_3 \rightarrow Fe(CO)_2(dmpe)(PMe_3) + CO \quad (8)$$

In conclusion, several important findings for ligand substitution processes at zero-valent iron centers have resulted from this research. First, $Fe(CO)_4PR_3$ complexes substitute CO with high quantum yield upon 337-nm photolysis with no appreciable substitution of PR_3. Second, $Fe(CO)_3(PR_3)_2$ complexes photosubstitute both PR_3 and CO although the quantum yield for substitution of PR_3 is very low. In either case, the intermediates formed upon CO dissociation react rapidly with trialkylphosphines. Third, as the number of coordinated phosphines increases from one to two, both the enthalpy of CO dissociation and subsequent phosphine addition become more endothermic in

---

[32] Hall, C.; Jones, W. D.; Mawby, R. J.; Osman, R.; Perutz, R. N.; Whittlsey, M. K. *J. Am. Chem. Soc.* **1992**, *114*, 7425.

[33] Siefert, E. E.; Angelici; R. J. *J. Organomet. Chem.* **1967**, *8*, 374.

[34] Smith, G. P. *Polyhedron* **1988**, *7*, 1605.

[35] The solvation enthalpy of reactants and products in organometallic reactions in organic solvents have been observed to be nearly equal and the net contribution to the enthalpy of reaction is nearly zero: (a) Bryndza, H. E.; Fong, L. K.; Paciello, R. A.; Tam, W.; Bercaw, J. E. *J. Am. Chem. Soc.* **1987**, *109*, 1444. (b) Bruno, J. W.; Marks, T. J.; Morss, L. R. *J. Am. Chem. Soc.* **1983**, *105*, 6824. (c) Gonzales, A. A; Zang, K.; Nolan, S. P.; de la Vega, R. L.; Mukerjee, S. L.; Hoff, C. D.; Kubas, G. J. *Organometallics* **1988**, *12*, 2429.

[36] Saillard, J.-Y.; Hoffmann, R. J. *J. Am. Chem. Soc.* **1984**, *106*, 2006.

[37] Braterman, P. S. In *Reactions of Coordinated Ligands*; Braterman, P. S., Ed.; Plenum: New York, 1986; Vol. 1, Chapter 1.

[38] Nayak, S. K.; Burkey, T. J. *Organometallics* **1991**, *10*, 3745.

[39] Computational investigations of alkane adducts of transition-metal complexes are underway. Cundari, T. Unpublished results (Chemistry Department MSU).

[40] Martin, L. A.; Einstein, F. W. B.; Pomeroy, R. K. *Inorg. Chem.* **1985**, *24*, 2777.

cyclohexane. Fourth, the $Fe(CO)_3(PR_3)$–PR_3 bond is as strong or stronger than the $Fe(CO)_3(PR_3)$–CO bond, but the $Fe(CO)_2(PR_3)_2$–PR_3 bond is weaker than the $Fe(CO)_2(PR_3)_2$–CO bond, a result inconsistent with arguments based on simple electronic structural effects. Taken as a whole these results point to the importance of steric factors in controlling the kinetics and thermodynamics of ligand substitution processes at reactive metal centers.

Acknowledgment. We thank Dr. Jean Rudzki Small for generously providing MQ software and documentation. The donors of the Petroleum Research Fund, administered by the American Chemical Society, and a Memphis State University Faculty Research Grant are acknowledged for partial support of this research.

Supplementary Material Available: Tables giving infrared carbonyl stretching frequencies and carbonyl ^{13}C NMR chemical shifts of iron carbonyl phosphines as well as ϕ_1, ϕ_2, and τ_2 determined for each complex at various ligand concentrations (4 pages). Ordering information is given on any current masthead page.